NOTES AND CORRESPONDENCE

An Approach to Kinetic Energy Diagnosis of Meso–Synoptic Scale Interactions

SHOU-JUN CHEN AND LE-SHENG BAI

Department of Geophysics, Peking University, Beijing, China

ERNEST C. KUNG

Department of Atmospheric Science, University of Missouri-Columbia, Columbia, Missouri

10 November 1989 and 6 June 1990

ABSTRACT

To explicitly describe the energy exchange between meso and synoptic-scale motions, a diagnostic scheme of kinetic energy has been developed. By using a horizontal filtering technique, meteorological variables are separated into synoptic and mesoscale components. A set of budget equations are derived for the kinetic energy $\hat{K}$ of synoptic scale motion $\hat{\mathbf{V}}$, the kinetic energy K' of mesoscale motion $\mathbf{V}'$, and the scalar product $\hat{\mathbf{V}} \cdot \mathbf{V}'$.

The scheme is applied to diagnose a severe rainstorm case over northern China during summer. The results show that the scale interactions between wind and height fields produce $\hat{\mathbf{V}} \cdot \mathbf{V}'$, which transfers kinetic energy to $\hat{K}$ and K'. The term $\hat{\mathbf{V}} \cdot \mathbf{V}'$ thus acts as a medium in scale interactions, conveying the energy between meso- and synoptic-scale motions and the potential energy source residing in the mass field.

1. Introduction

Interaction between synoptic and mesoscale circulation systems has been a point of interest in the observational diagnosis of the atmosphere. Maddox (1980a) and Maddox and Doswell (1982), using the rawinsonde observations, indicated the existence of a mesoscale high in the storm complex. The upper flow is split and diverged around the main convective system and the jet stream is accelerated owing to the increasing pressure gradient north of the mesohigh. To diagnose the local scale interactions Holopainen and Nurmi (1979, 1980) used a horizontal filtering technique to decompose the flow into large-scale and subgrid-scale components, and a stress term was introduced in the equation of large-scale motion. With data over northern Europe under a strong diffluent jet stream, they found that the flow is accelerated by the horizontal subgrid-scale force. Using a similar method, Chen and Xie (1982) obtained a kinetic energy equation to account for scale interactions, and diagnosed two rainstorm cases. Their results showed that the subsynoptic-scale motion transfers the kinetic energy to the synoptic-scale motion in the upper troposphere, and the synoptic-scale motion to the subsynoptic-scale motion in the lower troposphere.

Carney and Vincent (1986a,b) developed a set of kinetic energy equations that may describe the interactions between synoptic and subsynoptic scale. The kinetic energy is partitioned into components representing synoptic-scale motion, δ-scale motion (which is the difference between the total and synoptic-scale flow), and interactions between the two scales. The Eulerian form of total kinetic energy budget equation was used to diagnose the influence of organized deep convective activity on the large scale flow during AVE/SESAME I, 10–11 April 1979. Their results indicate the importance of scale interaction in the horizontal advective term after the occurrence of intense convection.

In this paper, a set of kinetic energy equations is developed by applying Holopainen and Nurmi's horizontal filtering technique (1979, 1980). The form of the resulting equations differs from that of Carney and Vincent's (1986a), in which the total and synoptic scales of motion are described by separate equations of motion without a scale interaction term for the synoptic scale equation. The equations in this study are developed so that the processes occurring between meso and synoptic-scale motions may be examined explicitly through energy transformations between these two scale ranges. The scheme was then applied to examine the case of a heavy rainstorm over northern China.

2. Kinetic energy equations

If we define a dummy meteorological variable A, in which a high-frequency portion of the field is filtered

Corresponding author address: Prof. Ernest C. Kung, Department of Atmospheric Science, University of Missouri-Columbia, Columbia, MO 65211.

by a designed objective analysis scheme, A can be expressed as:

$$A = \hat{A} + A', \tag{1}$$

where the caret ($\hat{}$) is a low-pass filter operator that retains synoptic-scale motion, and the prime ($'$) is a band-pass filter for mesoscale waves. The horizontal momentum equation can be written as

$$\frac{\partial \mathbf{V}}{\partial t} + (\mathbf{V}\cdot\nabla)\mathbf{V} + \omega\frac{\partial \mathbf{V}}{\partial p} = -\nabla\phi - \mathbf{k}f\times\mathbf{V} + \mathbf{F}, \tag{2}$$

where $\mathbf{V}$ is the vector of the horizontal wind, ϕ the geopotential height, ω the vertical p-velocity, $\mathbf{k}$ the vertical unit vector, f the Coriolis parameter, and $\mathbf{F}$ the frictional force. Taking the scalar product of (2) and $\mathbf{V}$ we obtain the kinetic energy equation

$$\frac{\partial K}{\partial t} + \mathbf{V}\cdot\nabla K + \omega\frac{\partial K}{\partial p} = -\mathbf{V}\cdot\nabla\phi + \mathbf{V}\cdot\mathbf{F}, \tag{3}$$

where $K = (\mathbf{V}\cdot\mathbf{V})/2$ is the total kinetic energy per unit mass, $\mathbf{V}\cdot\nabla K$ and $\omega(\partial K/\partial p)$ the horizontal and vertical advection of kinetic energy, $-\mathbf{V}\cdot\nabla\phi$ the cross-contour generation of kinetic energy, and $\mathbf{V}\cdot\mathbf{F}$ the dissipation.

According to the definition (1), the total wind components $\mathbf{V}$, geopotential height ϕ, and friction force $\hat{\mathbf{F}}$ can be expressed as

$$\mathbf{V} = \hat{\mathbf{V}} + \mathbf{V}', \tag{4}$$

$$\phi = \hat{\phi} + \phi', \tag{5}$$

$$\mathbf{F} = \hat{\mathbf{F}} + \mathbf{F}'. \tag{6}$$

By means of (4), the total kinetic energy can be partitioned into

$$K = \hat{K} + K' + \hat{\mathbf{V}}\cdot\mathbf{V}', \tag{7}$$

where $\hat{K} = (\hat{\mathbf{V}}\cdot\hat{\mathbf{V}})/2$ is the synoptic-scale kinetic energy, $K' = (\mathbf{V}'\cdot\mathbf{V}')/2$ is the mesoscale kinetic energy, and $\hat{\mathbf{V}}\cdot\mathbf{V}'$ is the scalar product of synoptic and mesoscale wind fields. The sign of $\hat{\mathbf{V}}\cdot\mathbf{V}'$ is determined by the angle α between $\hat{\mathbf{V}}$ and $\mathbf{V}'$. If $-\pi/2 < \alpha < \pi/2$, then $\hat{\mathbf{V}}\cdot\mathbf{V}'$ is positive, which means the total kinetic energy is the sum of $\hat{K}$, K' and $\hat{\mathbf{V}}\cdot\mathbf{V}'$. If $\pi/2 < \alpha < 3\pi/2$, then $\hat{\mathbf{V}}\cdot\mathbf{V}'$ is negative, and the sum of $\hat{K}$ and K' is reduced by $\hat{\mathbf{V}}\cdot\mathbf{V}'$. The term $\hat{\mathbf{V}}\cdot\mathbf{V}'$ is the part of kinetic energy contributed by both synoptic and mesoscale motions. It is also noted that the horizontal and vertical advections of kinetic energy in (3) can be partitioned into those of $\hat{K}$, K' and $\hat{\mathbf{V}}\cdot\mathbf{V}'$:

$$\mathbf{V}\cdot\nabla K = \mathbf{V}\cdot\nabla\hat{K} + \mathbf{V}\cdot\nabla K' + \mathbf{V}\cdot\nabla(\hat{\mathbf{V}}\cdot\mathbf{V}'), \tag{8}$$

$$\omega\frac{\partial K}{\partial p} = \omega\frac{\partial \hat{K}}{\partial p} + \omega\frac{\partial K'}{\partial p} + \omega\frac{\partial \hat{\mathbf{V}}\cdot\mathbf{V}'}{\partial p}. \tag{9}$$

Applying the low-pass filter to (2), we obtain

$$\frac{\partial \hat{\mathbf{V}}}{\partial t} + \widehat{(\mathbf{V}\cdot\nabla)\mathbf{V}} + \omega\widehat{\frac{\partial \mathbf{V}}{\partial p}} = -\nabla\hat{\phi} - \mathbf{k}f\times\hat{\mathbf{V}} + \hat{\mathbf{F}}. \tag{10}$$

Equation (10) can be rewritten as

$$\frac{\partial \hat{\mathbf{V}}}{\partial t} + (\mathbf{V}\cdot\nabla)\hat{\mathbf{V}} + \omega\frac{\partial \mathbf{V}}{\partial p} = -\nabla\hat{\phi} - \mathbf{k}f\times\hat{\mathbf{V}} + \hat{\mathbf{F}} + \mathbf{I} + \mathbf{J}, \tag{11}$$

where

$$\mathbf{I} = -\widehat{[(\mathbf{V}\cdot\nabla)\mathbf{V} - (\mathbf{V}\cdot\nabla)\hat{\mathbf{V}}]}, \tag{12}$$

and

$$\mathbf{J} = -\left(\omega\widehat{\frac{\partial \mathbf{V}}{\partial p}} - \omega\frac{\partial \hat{\mathbf{V}}}{\partial p}\right), \tag{13}$$

represent the horizontal and vertical "stress" of the mesoscale motion on the synoptic motion, respectively (Holopainen and Nurmi 1979).

The momentum equation for the mesoscale can be obtained by subtracting the synoptic scale (11) from the momentum (2):

$$\frac{\partial \mathbf{V}'}{\partial t} + (\mathbf{V}\cdot\nabla)\mathbf{V}' + \omega\frac{\partial \mathbf{V}'}{\partial p} = -\nabla\phi' - \mathbf{k}f\times\mathbf{V}' + \mathbf{F}' - \mathbf{I} - \mathbf{J}. \tag{14}$$

Taking the scalar product of (11) and $\hat{\mathbf{V}}$, the kinetic energy equation for synoptic-scale motion may be written as

$$\frac{\partial \hat{K}}{\partial t} + \mathbf{V}\cdot\nabla\hat{K} + \omega\frac{\partial \hat{K}}{\partial p} = -\hat{\mathbf{V}}\cdot\nabla\hat{\phi} + \hat{\mathbf{V}}\cdot\hat{\mathbf{F}} + \mathbf{I}\cdot\hat{\mathbf{V}} + \mathbf{J}\cdot\hat{\mathbf{V}}. \tag{15}$$

The mesoscale kinetic energy equation can then be obtained by taking the scalar product of (14) and $\mathbf{V}'$:

$$\frac{\partial K'}{\partial t} + \mathbf{V}\cdot\nabla K' + \omega\frac{\partial K'}{\partial p} = -\mathbf{V}'\nabla\phi' + \mathbf{F}'\cdot\mathbf{V}' - \mathbf{I}\cdot\mathbf{V}' - \mathbf{J}\cdot\mathbf{V}'. \tag{16}$$

The local time change of $\hat{\mathbf{V}}\cdot\mathbf{V}'$ can be written as

$$\frac{\partial \hat{\mathbf{V}}\cdot\mathbf{V}'}{\partial t} = \hat{\mathbf{V}}\cdot\frac{\partial \mathbf{V}'}{\partial t} + \mathbf{V}'\cdot\frac{\partial \hat{\mathbf{V}}}{\partial t}. \tag{17}$$

Introducing (11) and (14) into (17), we obtain the budget equation of $\hat{\mathbf{V}}\cdot\mathbf{V}'$ as

$$\frac{\partial \hat{\mathbf{V}}\cdot\mathbf{V}'}{\partial t} + \mathbf{V}\cdot\nabla(\hat{\mathbf{V}}\cdot\mathbf{V}') + \omega\frac{\partial \hat{\mathbf{V}}\cdot\mathbf{V}'}{\partial p} = -(\mathbf{V}'\cdot\nabla\hat{\phi} + \hat{\mathbf{V}}\cdot\nabla\phi') + \hat{\mathbf{F}}\cdot\mathbf{V}' + \mathbf{F}'\cdot\hat{\mathbf{V}} - \mathbf{I}\cdot\hat{\mathbf{V}} - \mathbf{J}\cdot\hat{\mathbf{V}} + \mathbf{I}\cdot\mathbf{V}' + \mathbf{J}\cdot\mathbf{V}'. \tag{18}$$

The following transformation functions may be defined:

$$\langle\hat{\mathbf{V}}\cdot\mathbf{V}', \hat{K}\rangle_h = \mathbf{I}\cdot\hat{\mathbf{V}}, \tag{19}$$

$$\langle\hat{\mathbf{V}}\cdot\mathbf{V}', \hat{K}\rangle_v = \mathbf{J}\cdot\hat{\mathbf{V}}, \tag{20}$$

$$\langle \hat{\mathbf{V}} \cdot \mathbf{V}', K' \rangle_h = -\mathbf{I} \cdot \mathbf{V}', \quad (21)$$

$$\langle \hat{\mathbf{V}} \cdot \mathbf{V}', K' \rangle_v = -\mathbf{J} \cdot \mathbf{V}', \quad (22)$$

where subscripts h and v denote the transformations by the horizontal and vertical motions. Positive values of transformation functions contribute to a decrease of $\hat{\mathbf{V}} \cdot \mathbf{V}'$ and an increase of $\hat{K}$ or K', meaning that the $\hat{\mathbf{V}} \cdot \mathbf{V}'$ is transformed to $\hat{K}$ or K'. Negative values indicate a reversed direction of the transfer. The following symbols are used for kinetic energy generation terms:

$$\text{GKS} = -\hat{\mathbf{V}} \cdot \nabla \hat{\phi}, \quad (23)$$

$$\text{GKM} = -\mathbf{V}' \cdot \nabla \phi', \quad (24)$$

$$\text{GKMS} = -(\mathbf{V}' \cdot \nabla \hat{\phi} + \hat{\mathbf{V}} \cdot \nabla \phi'). \quad (25)$$

The term GKS is the generation of synoptic-scale kinetic energy by the synoptic-scale cross-contour flow relative to the synoptic scale height, and the term GKM is the generation of mesoscale kinetic energy by the mesoscale cross-contour flow relative to the mesoscale height. GKMS represents the kinetic energy generated by the cross-contour interactions; i.e., the mesoscale wind crossing the synoptic-scale contours and the synoptic-scale wind crossing mesoscale contours.

The budget equations (15), (16), and (18) for $\hat{K}$, K', and $\hat{\mathbf{V}} \cdot \mathbf{V}'$ thus can be rewritten as

$$\frac{\partial \hat{K}}{\partial t} + \mathbf{V} \cdot \nabla \hat{K} + \omega \frac{\partial \hat{K}}{\partial p} = GKS + \langle \hat{\mathbf{V}} \cdot \mathbf{V}', \hat{K} \rangle_h + \langle \hat{\mathbf{V}} \cdot \mathbf{V}', \hat{K} \rangle_v + \hat{\mathbf{V}} \cdot \hat{\mathbf{F}}, \quad (26)$$

$$\frac{\partial K'}{\partial t} + \mathbf{V} \cdot \nabla K' + \omega \frac{\partial K'}{\partial p} = GKM + \langle \hat{\mathbf{V}} \cdot \mathbf{V}', K' \rangle_h + \langle \hat{\mathbf{V}} \cdot \mathbf{V}', K' \rangle_v + \mathbf{V}' \cdot \mathbf{F}', \quad (27)$$

$$\frac{\partial \hat{\mathbf{V}} \cdot \mathbf{V}'}{\partial t} + \mathbf{V} \cdot \nabla (\hat{\mathbf{V}} \cdot \mathbf{V}') + \omega \frac{\partial \hat{\mathbf{V}} \cdot \mathbf{V}'}{\partial p} = GKMS + \hat{\mathbf{V}} \cdot \mathbf{F}' + \mathbf{V}' \cdot \hat{\mathbf{F}} - \langle \hat{\mathbf{V}} \cdot \mathbf{V}', \hat{K} \rangle_h - \langle \hat{\mathbf{V}} \cdot \mathbf{V}', \hat{K} \rangle_v - \langle \hat{\mathbf{V}} \cdot \mathbf{V}', K' \rangle_h - \langle \hat{\mathbf{V}} \cdot \mathbf{V}', K' \rangle_v. \quad (28)$$

The kinetic energy (3) may be obtained as the summation of (26)–(28).

In (26)–(28), two types of energy source terms are seen. First, the synoptic-scale kinetic energy and mesoscale kinetic energy are produced or destroyed in the wind and pressure fields by the cross-contour motion in the same scale range. Thus, neither synoptic-scale motion $\mathbf{V}$ nor mesoscale motion $\mathbf{V}'$ can gain or lose kinetic energy from scale interactions between wind and mass of different scale ranges. As shown in (28), GKMS, the first term on the right-hand side, is the kinetic energy production through an interaction between meso and synoptic-scale wind and height fields, but it only produces $\hat{\mathbf{V}} \cdot \mathbf{V}'$. The potential energy residing in the mass field during the scale interactions is transformed to $\hat{\mathbf{V}} \cdot \mathbf{V}'$ rather than directly to $\hat{K}$ or K'. Second, although there is no direct kinetic energy transfer between synoptic and mesoscale motions, the exchanges between $\hat{K}$ and K' can be accomplished through $\hat{\mathbf{V}} \cdot \mathbf{V}'$ as described in (19)–(22). These transformation processes in the meso and synoptic-scale motions are demonstrated by a block diagram in Fig. 1. The term $\hat{\mathbf{V}} \cdot \mathbf{V}'$ acts as a medium between synoptic and mesoscale motions.

It should be noted that the terms at the left-hand sides of (26)–(28) are the total time changes of $\hat{K}$, K', and $\hat{\mathbf{V}} \cdot \mathbf{V}'$, which represent the kinetic energy budget of a moving air parcel. Thus, the above discussions account for the kinetic energy budget of a moving volume of the atmosphere; i.e., the quasi-Lagrangian form as described by Vincent and Chang (1975). For the Eulerian form of energy description the contribution of horizontal and vertical advection terms must be included.

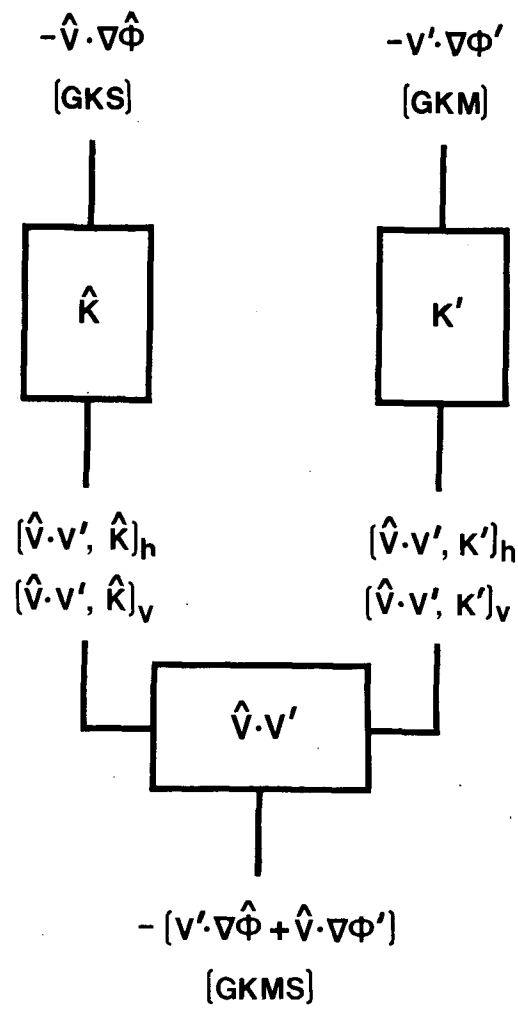

FIG. 1. Block diagram for the meso and synoptic-scale kinetic energy flow. Symbols are as defined in the text.

3. Evaluation of scale interactions for a rainstorm case

The budget equations developed in section 2 can be applied to any dataset in which different scales of motion are resolvable. For the conventional twice-daily upper-air sounding in China, the average spacing between stations is 300 km. This only allows a resolution for the meso-α scale features. The horizontal scale of rainstorms in China during the summer ranges from 500 to 1500 km, and thus a severe rainstorm case is chosen to examine its scale interactions.

Heavy rainstorms occurred during 0000–1200 UTC 26 July 1977, with maximum precipitation up to 150 mm within 12 h over northern China. The rainfall area oriented from the Hebei province (32°N, 115°E) to the Jilin province (43°N, 125°E), which was 300 km wide and 1000 km long (Fig. 2a). The domain of analysis is 32°–47°N and 109°–127°E with 42 rawinsonde observations in the area. The soundings are checked vertically using the hydrostatic relationship. Obvious errors in records, such as displacement of variables and misplaced order of magnitude, were properly corrected. Other values that failed in the hydrostatic check were eliminated. Barnes' (1964, 1973) objective analysis scheme was then used to produce values on a grid with 100-km spacing. The gridpoint vertical velocity is calculated using the kinematic method, involving O'Brien's (1970) corrective scheme with the vertically integrated divergence adjusted for $\omega = 0$ at the surface and 100 mb.

To decompose the synoptic and mesoscale features, Maddox's (1980b) method, based on Barnes' scheme, is used. The response function for Barnes' scheme is given by

$$R = R_0(1 + R_0^{g-1} - R_0^{g}) \tag{29}$$

where R is the final response, $R_0 = \exp(-4\pi^2 c/\lambda^2)$, λ the wavelength, and g and c the parameters of the scheme. Let A be the variable, and $\hat{A}$ be the low pass analysis from which the synoptic variables are resolved. The response functions referred to as R and $\hat{R}$ are illustrated in Fig. 2. The band-pass field A' is given by

$$A' = \eta(A - \hat{A}), \tag{30}$$

and the band-pass filter response R' is

$$R' = \eta(R - \hat{R}), \tag{31}$$

where η is a normalization factor (taken as 1.05 in this case) assigned the value of the reciprocal of the maximum value of $(R - \hat{R})$. Band-pass response is restored to 100% at the wavelength (λ_{max}) where maximum difference occurs. The response curve R with $g = 0.25$ and $c = 9500$ in Fig. 2 shows that about 60% of the amplitude with a 500-km wavelength is resolved. In order to produce a consistent field of synoptic variables from which the bandpass response would be in the mesoscale region, the values of c and g are taken as 0.45 and 250 000. The response curve $\hat{R}$ shows that

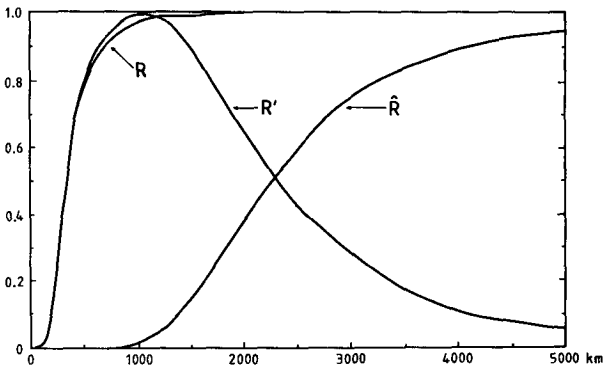

FIG. 2. Response curves as functions of wavelength. Curves R and $\hat{R}$ are for the low-pass filters that define total and synoptic meteorological fields. Curve R' is the response of band-pass (mesoscale) filter ($\eta = 1.05$).

about a 60% signal of the wavelength at 2500 km is resolved. The response curve R' for the mesoscale has a peak at wavelength 1000 km and an average response of 80% between 500 and 2000 km.

Figure 3(a–d) depicts the synoptic and mesoscale wind fields at 850 and 200 mb. The original data points are shown in Fig. 4a. Heavy precipitation is located to the northwest of the western Pacific anticyclone. In the synoptic-scale flow, a strong low-level current from the East China Sea is directed to the rainfall area, transporting warm moist air. At 200 mb the storm is located 500 km east of a major trough in the right-rear quadrant of the jet streak where the divergence dominates (see Palmen and Newton 1969). This synoptic environment is similar to the configuration for severe thunderstorms over North America as presented by Beebe and Bates (1955). A mesolow and mesohigh at Liaoning province (42°N, 121°E) and the northern Bohai Sea (40°N, 124°E) are evident on the 850-mb mesoscale map (Fig. 3c). The confluence zone between the mesolow and mesohigh coincides with the precipitation area. The mesolow and mesohigh can also be seen on the height map (Fig. 4a). At 200 mb (Fig. 3d), diffluent southwesterlies are recognized around the storm with a strong outflow at the northwest quadrant of the rainstorm area. This diffluent flow occurs between the mesohigh over the eastern portion of the Bohai Sea (38°N, 117°E) and the mesolow over the middle valley of the Yellow River (37°N, 112°E) (Fig. 4b). Similar diffluent flow in the upper troposphere over the storm area was also noted by Maddox's study (1980a).

In the diagnostic domain as shown in Fig. 3c, the mesolow with the lower-level confluence zone and the upper level diffluent flow are enclosed. Figure 5a shows the vertically integrated area-averaged generation terms and the interaction terms for 0000–1200 UTC 26 July 1977. The total generation ($GK = GKS + GKM + GKMS$) is positive and reaches 9.7 W m^{-2}, which is consistent in order of magnitude with the energetic

studies of the convective environment over North America (Kung and Tsui 1975) under the severe storm condition. The profile of total generation in Fig. 6a shows two peaks, one in the planetary boundary layer and the other, much larger one, in the upper troposphere. This feature is also similar to what was observed by Kung and Tsui.

Among the three generation terms, the contribution of GKMS is the largest. Similar results have been obtained by Carney and Vincent (1986) in the deep convective area during AVE/SESAME I 10–11 April 1979. However, it is important to note that GKMS only produces $\hat{\mathbf{V}} \cdot \mathbf{V}'$. The GKMS depends upon the orientation of the synoptic and mesoscale winds with respect to the gradient of the meso and synoptic-scale height fields. Two peaks of GKMS in the troposphere appear at similar levels to those of the total generation (Fig. 6a). The mesoscale generation GKM acts as another source of energy, but its value is much smaller than that of GKMS. The vertical total of the synoptic-scale generation GKS is negative. This destruction of kinetic energy occurs in the midtroposphere, whereas in the

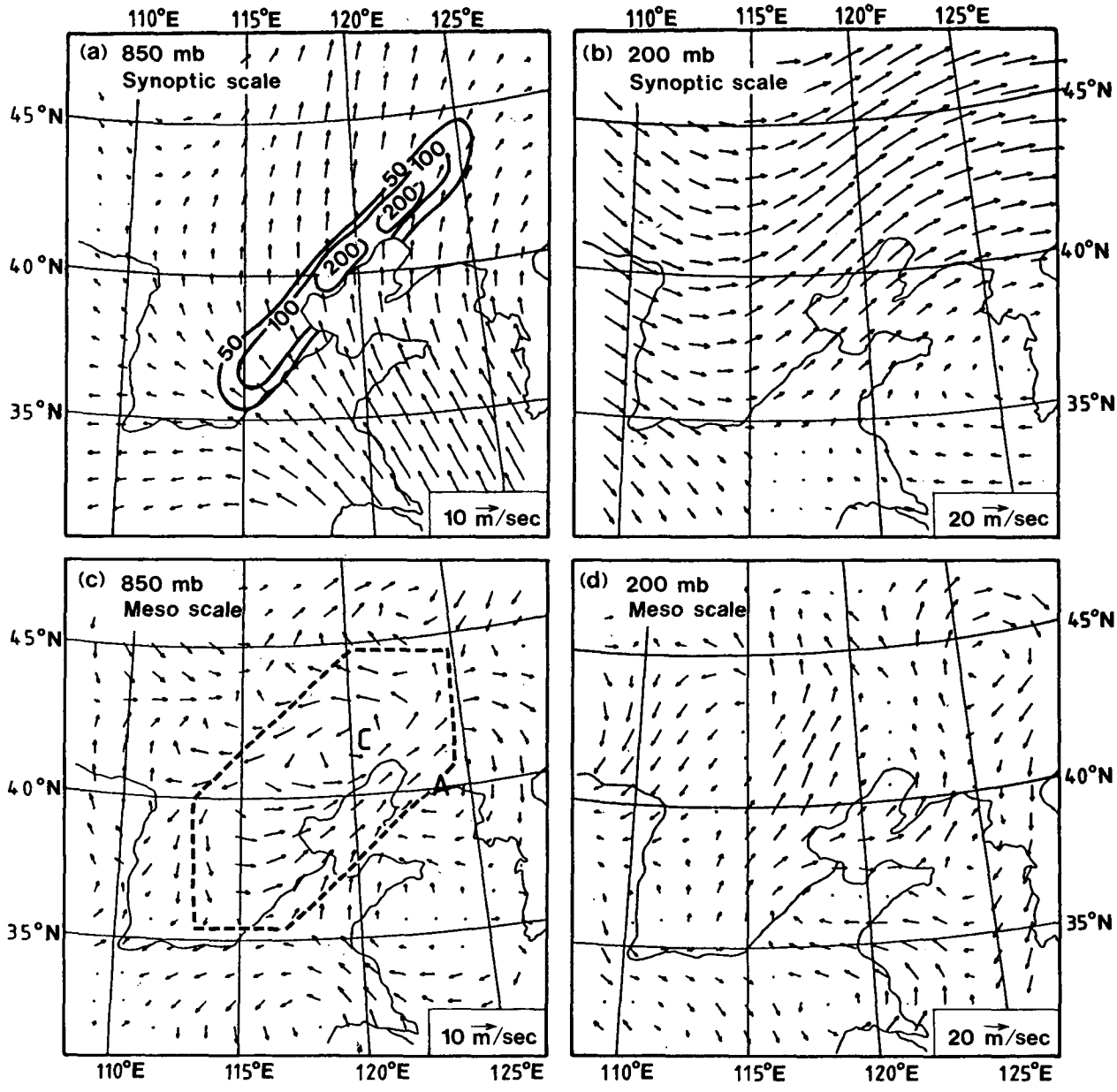

FIG. 3. Wind analysis at 1200 UTC 26 July 1977. (a) Synoptic scale at 850 mb. Solid lines indicate the rainfall during 0000–1200 UTC in unit of mm. (b) Synoptic scale at 200 mb. (c) Mesoscale at 850 mb. Heavy dashed line encloses the diagnosis area. (d) Mesoscale at 200 mb.

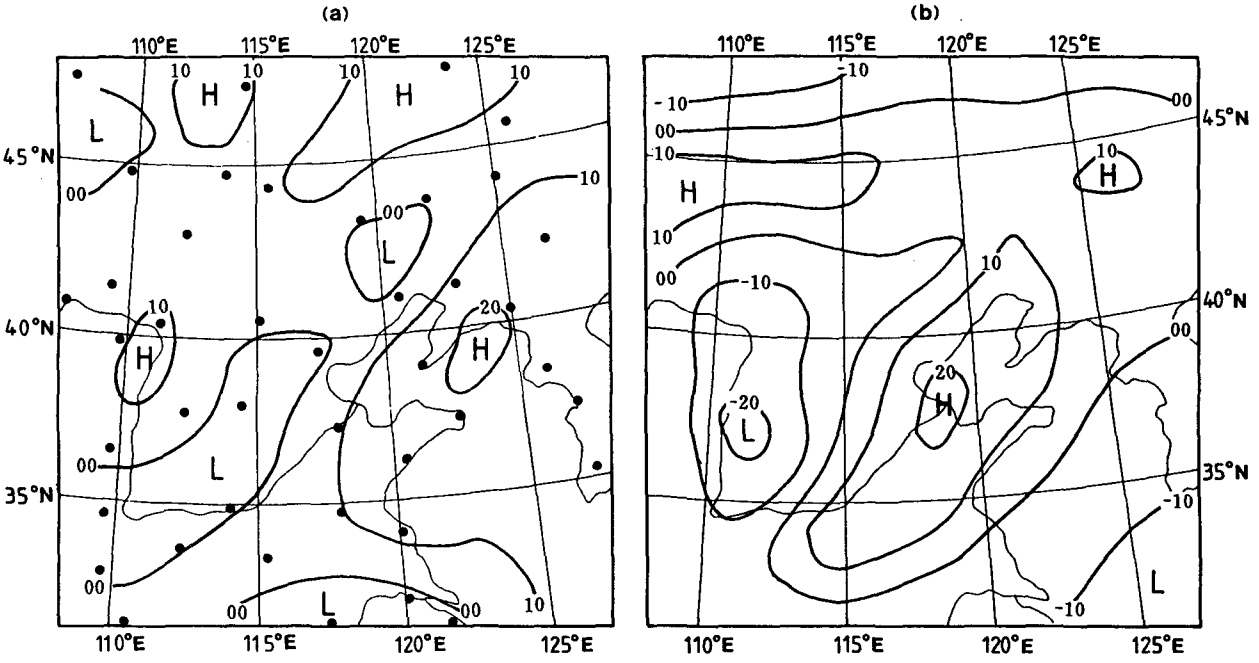

FIG. 4. Mesoscale height analysis at 1200 UTC 26 July 1977. (a) 850 mb. (b) 200 mb. Height contours in every 10 gpm. Original data points are shown in (a).

upper and lower troposphere GKS is positive. The magnitude of mesoscale generations GKM is much smaller than that of GKS, but also shows a peak in the upper troposphere (Fig. 6b).

The kinetic energy transfers by horizontal motions, $\langle \hat{\mathbf{V}} \cdot \mathbf{V}', \hat{K} \rangle_h$ and $\langle \hat{\mathbf{V}} \cdot \mathbf{V}', K' \rangle_h$, are positive, and in the same magnitude as those of the generation terms. The transfers by the vertical motion $\langle \hat{\mathbf{V}} \cdot \mathbf{V}', \hat{K} \rangle_v$ and $\langle \hat{\mathbf{V}} \cdot \mathbf{V}', \hat{K} \rangle_v$ are negative, but they are only one-third of those of the horizontal transfers. The horizontal transfers are the dominant part of the total transfer, and the total transfers have the same sign as those of the horizontal transfers. It is apparent that the $\hat{\mathbf{V}} \cdot \mathbf{V}'$ transfers kinetic energy to $\hat{K}$ and K' through horizontal motion in this storm case. Figures 4b and 6 also indicate that the major interactions between synoptic and mesoscale motions occur in the upper troposphere.

4. Remarks

The so-called mesoscale motion covers a wide scale range between the synoptic and microscale motions. Although the budget equations in this study are applicable to any dataset, the scale range and phenomena isolated are very much dependent on the scale of the observation network and filtering technique employed. The scale of motion isolated in this study is clearly subsynoptic, but at the vicinity of the synoptic scale. However, it is encouraging that a distinctly different scale of motion from the synoptic scale is obtained in this preliminary study. It will be worthwhile to extend this study with the datasets of a finer observation network. It will also be interesting to apply the present method to the available potential energy to obtain a complete set of equations.

Budget equations are developed in this paper from equations of motion for the synoptic and mesoscale motions that are consistent with each other in reference to the scale interaction terms. The most interesting point may be the role of the scalar product $\hat{\mathbf{V}} \cdot \mathbf{V}'$ in the kinetic energy processes, which may give some in-

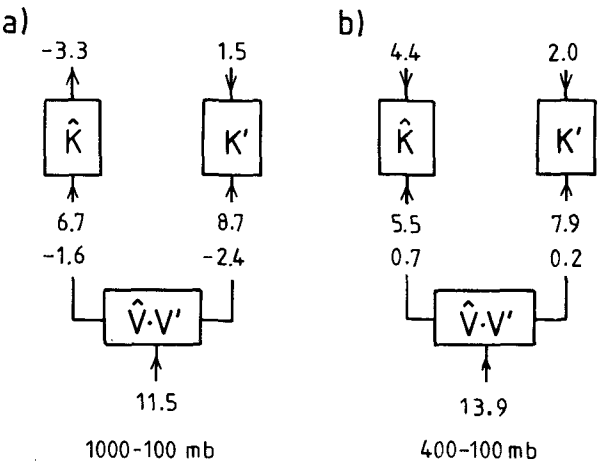

FIG. 5. (a) 1000–100 mb kinetic energy transformations in the diagnosis area shown in Fig. 3c during 0000–1200 UTC 26 July 1977. Units are in W m^{-2}. (b) As in (a) but for 400–100 mb.

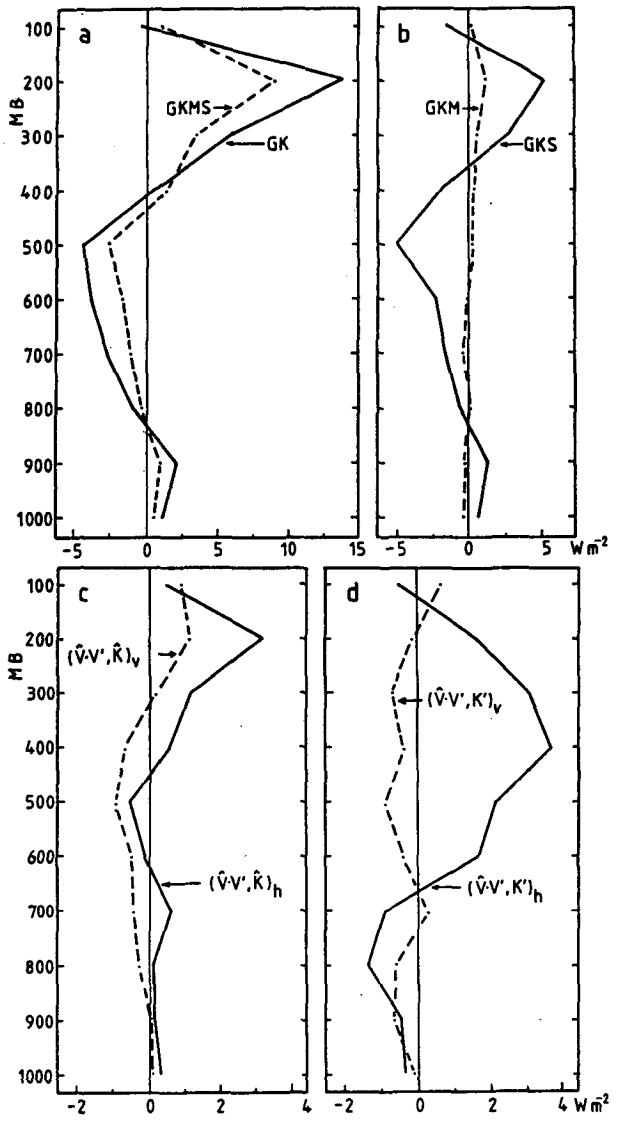

FIG. 6. (a) Vertical profiles of total generation (solid line) and GKMS (dashed line) in the storm area. (b) As in (a) but for the GKS (solid line) and GKM (dashed line). (c) As in (a) but for the $\langle \hat{\mathbf{V}} \cdot \mathbf{V}', \hat{K} \rangle_h$ (solid line) and $\langle \hat{\mathbf{V}} \cdot \mathbf{V}', \hat{K} \rangle_v$ (dashed line). (d) As in (a) but for the $\langle \hat{\mathbf{V}} \cdot \mathbf{V}', \hat{K} \rangle_h$ (solid line) and $\langle \hat{\mathbf{V}} \cdot \mathbf{V}', K' \rangle_v$ (dashed line).

sight to scale interactions. It obtains energy from the source of potential energy in the synoptic and mesoscale fields and conveys it to the synoptic and mesoscale motions. The term $\hat{\mathbf{V}} \cdot \mathbf{V}'$ thus acts as a medium in the energy transfer between synoptic and mesoscale motions. Its physical interpretation is not yet clear, although we may conceive a transfer process similar to the familiar microscale eddy transfer process among whirls of different size (e.g., Hess 1959). The existence of distinct patterns for the synoptic and mesoscale circulations (Figs. 3 and 4) may be mentioned in this regard. In any case it shows the complexity of the scale interactions whose processes are not yet well understood.

Acknowledgments. The authors are indebted to Professor E. Holopainen for his valuable comments, to Dr. S. L. Barnes for providing the objective analysis code, and to Professor F. Sanders and two anonymous reviewers whose constructive comments have led to significant improvement of this report. The technical assistance of D. K. Williams and G. D. Vickers is also gratefully acknowledged. This report, which is contribution Journal Series Number 10 962 from the Missouri Agricultural Experiment Station, was supported by the National Oceanic and Atmospheric Administration under Grant NA88AA-D-AC103.

REFERENCES

Barnes, S. L., 1964: A technique for maximizing details in numerical weather analysis. *J. Appl. Meteor.*, **3**, 396–409.

——, 1973: Mesoscale objective map analysis using weighted time-series observations. NOAA Tech. Memo. ERL NSSL 62, 60 pp. [NTIS COM-73-10781.]

Beebe, R. G., and F. C. Bates, 1955: A mechanism for assisting in the release of convective instability. *Mon. Wea. Rev.*, **83**, 1–10.

Carney, T. G., and D. G. Vincent, 1986a: Meso-synoptic scale interactions during AVE/SESAME I, 10–11 April 1979. Part I: Theoretical development of interaction equations. *Mon. Wea. Rev.*, **114**, 344–352.

——, and ——, 1986b: Meso-synoptic interactions during AVE/SESAME I, 10–11 April 1979. Part II: Influence of convective activity on large-scale flow. *Mon. Wea. Rev.*, **114**, 353–370.

Chen, S. J., and A. Xie, 1981: The exchange of kinetic energy between synoptic and subsynoptic-scale motions. *Acta. Meteor. Sinica.*, **39**, 405–415, (in Chinese).

Hess, S. L., 1959: *Introduction to Theoretical Meteorology.* Henry Holt and Co., 362 pp.

Holopainen, E., and P. Nurmi, 1979: Acceleration of a diffluent jet stream by horizontal subgrid-scale processes—an example of a scale-interaction study employing a horizontal filtering technique. *Tellus*, **31**, 346–353.

——, 1980: A diagnostic scale-interaction study employing a horizontal filtering technique. *Tellus*, **32**, 124–130.

Kung, E. C., and T. L. Tsui, 1975: Subsynoptic-scale kinetic energy balance in the storm area. *J. Atmos. Sci.*, **32**, 729–740.

Maddox, R. Z., 1980a: Mesoscale convective complexes. *Bull. Amer. Meteor. Soc.*, **61**, 1374–1387.

——, 1980b: An objective technique for separating macroscale and mesoscale features in meteorological data. *Mon. Wea. Rev.*, **108**, 1108–1121.

——, and C. A. Doswell III, 1982: An examination of jet stream configurations, 500-mb vorticity advection, and low-level thermal advection patterns during extended periods of intense convection. *Mon. Wea. Rev.*, **110**, 184–197.

O'Brien, J. J., 1970: Alternative solutions to the classical vertical velocity problem. *J. Appl. Meteor.*, **9**, 197–203.

Palmen, E., and C. W. Newton, 1969: *Atmospheric Circulation Systems.* Academic Press, 603 pp.

Vincent, D. G., and L. N. Chang, 1975: Kinetic energy budgets of moving systems: case studies for an extratropical cyclone and Hurricane Celia, 1970. *Tellus*, **27**, 215–233.